Journal of Design Against Fatigue
https://minerva-aset.com/JDAF
MINERVA ASET
ISSN 2976-940X

Failure strength of 7075-T6 aluminium alloy: integrating digital image and finite element analysis for static uniaxial and biaxial load scenarios

Ogunjobi Kehinde Emmanuel[1], Richard Nwawe Tchadeu[1], Fatemeh Marashi Najafi[2], Hossein Madani[3], Mahmoud Chizari[1]*

1 School of Physics Engineering and Computer Science, University of Hertfordshire, Hatfield, UK
2 Research Center for Advanced Materials, Faculty of Materials Engineering, Sahand University of Technology, Tabriz, Iran
3Jaguar Land Rover Ltd, Whitley, Coventry, UK

P A P E R I N F O

Paper history:
Received 2 October 2024
Received in revised form 3 November 2024
Accepted 6 November 2024

Keywords:
7075-T6 Aluminium alloy; Uniaxial and biaxial loads; Digital image correlation; Numerical and experimental simulations

A B S T R A C T

The objective of this study is to investigate the mechanical properties of 7075-T6 Aluminium (Al) alloy under both uniaxial and biaxial loads. The study will be conducted using a combination of experimental and numerical methods. The experimental method used is the digital image correlation (DIC) technique, which was utilized to capture the deformation and strain fields of the material specimen under tensile test. The tensile test can be significant due to the relation with the fatigue behaviour. Thus, a tensile machine was employed to apply uniaxial and biaxial loads on the sample. The strain and deformation distribution of the results was generated on the DIC and correlated software. The numerical method involved the use of a commercial finite element software to create a finite element model and simulate the mechanical behaviour of the material under the same loading conditions. The results obtained from the experimental and numerical methods were compared to validate the accuracy of the numerical model. The outcomes demonstrated that under uniaxial loading, localized necking and fracture were observed, while biaxial loading resulted in shear deformation and fracture. This research contributes to the development of more accurate models for predicting the mechanical behaviour of the model samples under different loading conditions.

https://doi.org/10.62676/jdaf.2024.2.2.20

1. INTRODUCTION·

Aluminium (Al) alloys, especially the 7075-T6 variant, are being considered as potential candidates for widespread applications in the automobile and aerospace industries [1–3]. This is primarily due to their superior features, including high strength to weight ratios, enhanced thermal and electrical conductivity, low density, cost-effectiveness, superb formability, and effective corrosion resistance [4–7]. The utilization of Al alloys in aerospace applications covers various parts, from structural components to engine parts, offering a balance between performance and economic viability [8–10]. Nevertheless, the Al alloys employed in automotive and aeronautical parts undergo a range of stress and loading conditions, which can significantly impact the life expectancy of the materials [11,12]. Therefore, a deep understanding of alloys characteristics and response under this stress situation is a crucial factor for optimizing component design, enhancing material performance, and preventing failure [13].

In other words, accurate knowledge of mechanical properties such as tensile strength, fatigue and fracture behaviour is vital for designing safe and efficient structures [14–16]. While substantial research has been conducted on the mechanical features of Al alloy under uniaxial loading conditions, where stresses are applied in a single direction, real-world applications often encompass more complex

·*Corresponding Author Email: m.chizari@herts.ac.uk . (Mahmoud Chizari)

Cite this article as: Ogunjobi Kehinde Emmanuel, Richard Nwawe Tchadeu, Fatemeh Marashi Najafi, Hossein Madani, Mahmoud Chizari, Failure strength of 7075-T6 aluminium alloy: integrating digital image and finite element analysis for static uniaxial and biaxial load scenarios, Journal of Design Against Fatigue, Vol. 2, No. 2, (2024) 13-21, https://doi.org/10.62676/jdaf.2024.2.2.20

loading circumstances as mentioned above. For instance, components in aircraft wings, fuselage structures, or high-performance automotive parts are under simultaneous uniaxial and biaxial loads, causing stress distributions that vary significantly from those under simple uniaxial cases [17]. Therefore, it becomes crucial to quantify the behaviour of 7075-T6 Al alloy under multidirectional loads to enable engineers to optimize and tailor material features for specific applications. Multidirectional loading can impact the tensile strength, which in turn influences the fatigue behaviour of the material. The results of various investigations have indicated the directed correlation of fatigue strength and tensile strength, while diverse studies have demonstrate the parabolic relation between two parameters[18,19]. This contraction can be due to the fact that diverse factors such as damage mechanism can impact the tensile and fatigue strength, which is different for both of them [20]. The results of literatures have demonstrated that tensile properties indicate the overall behaviour of a material, fatigue properties are often affected by local weaknesses such as micro-cracks and inclusions, which should be minimized. Moreover, the instability of microstructure cause local softening during cyclic loading. Thus, fatigue strength is a comprehensive reflection of both macroscopic tensile behaviour and microscopic damage conditions [21]. Previous investigations have reported valuable overviews into the mechanical behaviour of Al alloys under complex loading. For instance, Siddiqui et al. [22] performed an experimental and analytical evaluation of AA7475-T761 Al alloy under planar biaxial loading. It was reported, while the nucleation and growth were the initial failure mechanism under uniaxial tensile loading, biaxial loading led to both ductile and brittle fracture, including cleavage and facet failure. Similarly, Hashemian et al. [23] investigated the fracture behaviour of the forged Al 7075-T6 alloy under mixed-mode loading circumstances and demonstrated that the obtained yield stress increased with forge-induced deformation. Their finding also showed that the alloys exhibited promoted resistance under tensile loading compared to shear loading .

Additionally, Chaves et al. [24] assessed the fatigue life and crack growth direction of 7075-T6 Al alloy with a circular hole subjected to biaxial load. The results of this investigation have shown that for the three types of loading, the crack initiated near the point of maximum principal stress on the hole surface, and propagated along the maximum principal stress.

Based on these studies, the current research aims to comprehensively characterize the mechanical behaviour of 7075-T6 Al alloy subjected to simultaneous uniaxial and biaxial loads through the integration of sophisticated characterization techniques and experimental testing. To supply these perquisites, precise modelling and simulation of structures utilizing 7075-T6 Al alloys under various loading conditions can be favourable. The application of tensile testing along with Digital Image Correlation (DIC) will evaluate the material's strength, ductility, toughness, and precisely measure the strains during both uniaxial and biaxial tasting, respectively. The findings will elucidate the anisotropic properties of 7075-T6 Al under these loading conditions, facilitating the development of more accurate models for real-world applications. Also, the mechanical testing data can be directly integrated into finite element analysis (FEA) simulations for further behavioural prediction. It is worth mentioning that, while extensive research has been conducted on the uniaxial behaviour of these alloys, their response under complex loading situation remains relatively unexplored .

Ultimately, this research aims to provide insight into material selection, design optimisation and performance prediction to support reliable engineering applications.

2. EXPERIMENTAL PROCEDURE

2.1. Material and Sample Preparation

The material utilized in this study was 7075-T6 Aluminium alloy. For specimen preparation, the samples were subjected to abrasion and polishing utilizing silicon carbide paper, to eradicate the cutting trace along with surface oxides.

To ensure material homogeneity, all samples for both uniaxial and biaxial testing were sourced from the same batch of the material. The test specimens were machined in accordance with a specific in-house geometry design, from the work of Nwawe et al. [25-26]. The specimen general overview and dimensions can be viewed from Fig.1and Fig.2 respectively .

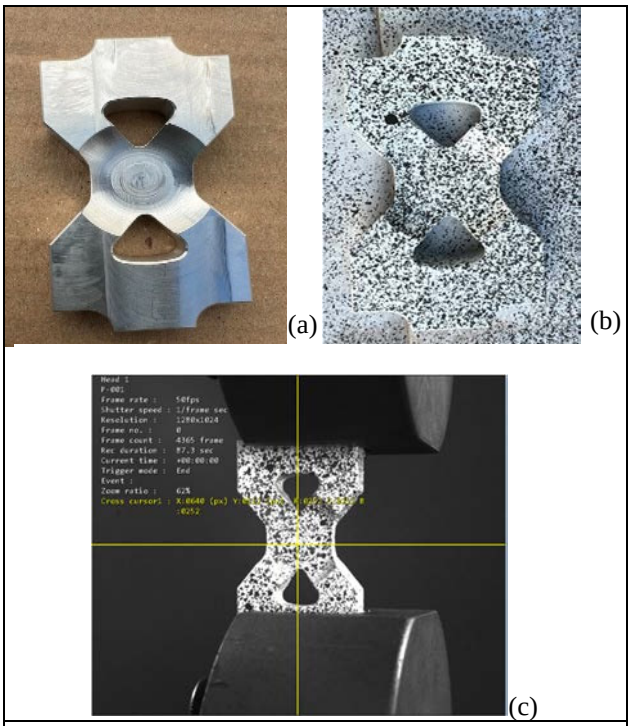

Fig 1. (a) Design 7075-T6 Aluminium specimen, (b) stochastic pattern speckled specimen, (c) captured image of test specimen on DIC camera.

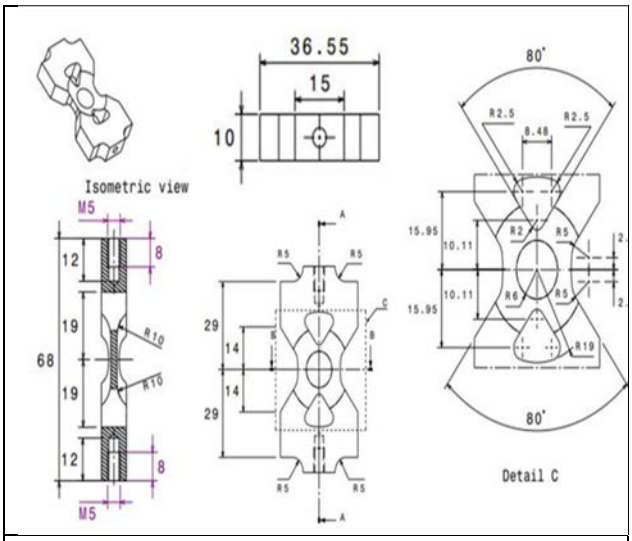

Fig. 2. Test specimen technical specification.

2.2. Uniaxial and Biaxial Loading Test

A Universal Testing Machine (UTM, Tinius Olsen, China) and the Digital Image Correlation (DIC) system were employed to investigate the mechanical behaviour on 7075-T6 Al alloy under axial and biaxial loading. The UTM applied axial and biaxial loads until specimen fracture, as illustrated in Fig. 3a. The test was conducted under constant strain rate with continuous strain measurement using strain gauges strategically placed to capture both longitudinal and transverse strains. UTM was employed to perform tensile tests under uniaxial and biaxial loads (16500N and 20100N) on standardized specimens with a gauge length of 66mm and a cross-sectional area of 176.79 mm². The data acquisition system recorded these measurements throughout the test and the corresponding strain data, maximum load and the associated strain at the fracture point were documented .

The DIC system, illustrated in Fig. 3b, and Fig. 4 (a, b, and c) provides full-field strain measurements by capturing the surface deformation of the specimens throughout the loading process. During the experiment, a random paint splatter pattern on the specimen surface provided unique markers for DIC software to track during deformation.

Stress-strain curves were generated for each test type, and material properties such as elastic modulus, yield strength, ultimate tensile strength, and ductility were extracted. The obtained results were meticulously examined and compared with existing literature to elucidate the behaviour of 7075-T6 Al under the investigated loading conditions.

The use of DIC improved measurement accuracy by correcting for lens distortion and relating image pixels to real-world distances. Additionally, DIC enabled accurate 3D reconstruction from multiple camera views .

2.2.1. DIC Calibration

GOM Correlate software package from the ZEISS Group, which uses Digital Image Correlation (DIC) to evaluate video files and digital image series from individual cameras, was used to visualise strain, deformation and displacement. Initially, the calibration plate featuring a high-precision pattern of circles or dots was employed to calibrate the DIC cameras, as shown in Fig.4d. The plate was positioned near the cameras, and the captured images were imported into the software. Corresponding points between the images and the digital model were manually aligned. This pre-calibration ensured that sufficient points were visible to both cameras, verifying the suitability of the test environment for accurate DIC analysis. Some key steps were implemented for DIC camera calibration using the calibration plate for camera positioning, including aperture and brightness optimization, lens focusing, field of view verification, and parameter estimation .

The cameras were equipped with appropriate lenses facing the region of interest (ROI) on the specimen, ensuring that all pre-calibration points were visible. Real-time camera views were established using the GOM software. For aperture and brightness optimization, the camera aperture was set to its minimum value, and brightness was adjusted to achieve optimal image exposure. To ensure precise lens focusing, a well-textured area on the specimen was used, with the camera lenses being zoomed in and out until the image, initially blurred, became sharp. In the next step, the final camera position was verified to confirm that the entire ROI and all pre-calibration points remained within the field of view. Finally, the known geometry of the calibration plate and the detected feature locations in the images were used to calculate the intrinsic camera parameters, including focal length, principal point (centre of distortion), and radial and tangential distortion coefficients. Following these steps guaranteed the capture of high-quality images suitable for subsequent DIC analysis.

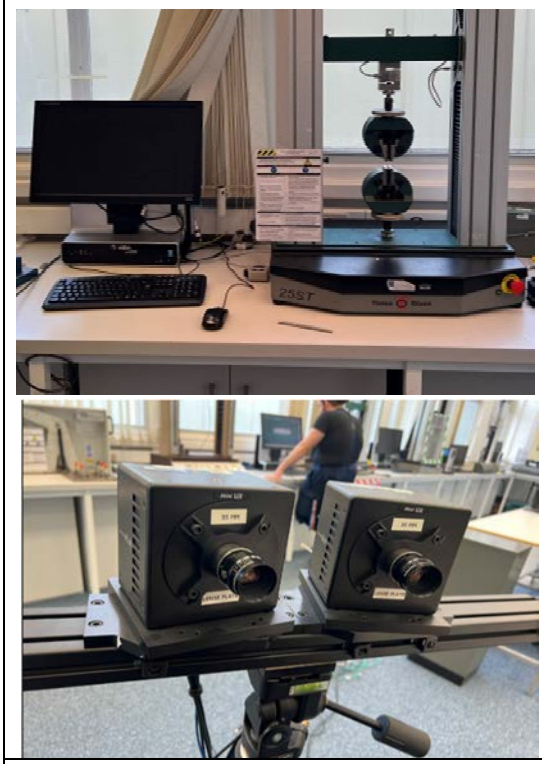

Fig 3. (a) Tinius-Olsen Universal Testing Machine utilized for the experiment, (b) DIC camera used for the experiment.

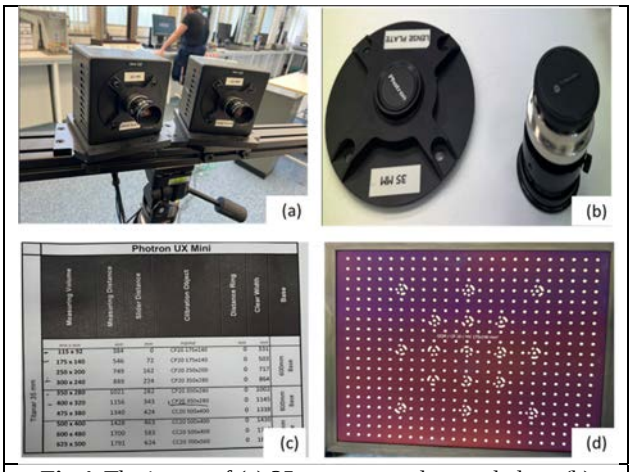

Fig 4. The image of (a) 35 mm camera lens and plate, (b) camera setup, (c) camera positioning configuration table, (d) GOM calibration plate.

2.2.2. DIC Camera Setup and Lighting Optimization

According to Fig. 5 (a-c), two DIC cameras were positioned at a distance of 384 mm to capture the entire speckled area of the specimen without overlap. Any potential obstructions were minimized to ensure a clear field of view. Prior to testing, the laboratory lighting was assessed and controlled to prevent variations due to external factors. To achieve this, skylights and windows were closed, dedicated lighting equipment was employed, and glare was minimized. Consistent and homogeneous illumination was achieved by positioning a lamp for direct lighting on the specimen. Live camera feeds were used to optimize lighting uniformity, by turning off extraneous room lighting during the test, and adjusting the camera aperture for appropriate image exposure.

2.2.3. DIC Data Post-Processing with GOM Correlate

GOM Correlate software was employed for the post-processing analysis of the DIC data. This software facilitates the extraction of key information from DIC experiments, including:

- Strain and displacement fields: GOM Correlate calculates these fields, providing detailed insight into material deformation under applied load.
- 3D deformation visualization: The software creates a visual representation of the material's deformation behaviour.
- Material property extraction: Material properties such as Young's modulus and Poisson's ratio can be retrieved for the design and evaluation process.
- Time-lapse analysis: This feature allows for studying deformation behaviour over time and identifying any variations.

The advanced capabilities of this software enabled a comprehensive analysis of the DIC data, providing valuable insights into the material's mechanical behaviour.

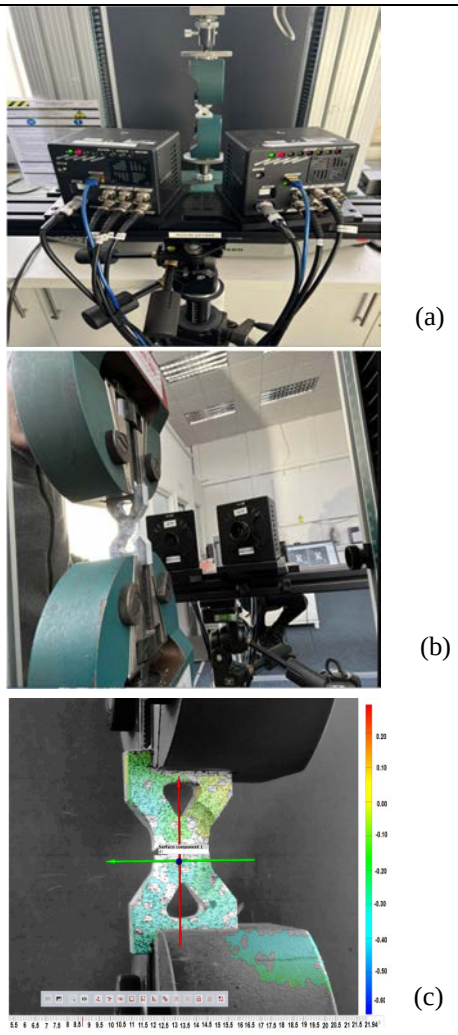

Fig 5. (a) Camera positioned at 384 mm from test specimen on the test machine, (b) Camera positioned and adjusted to test specimen set up, (c) Time-lapsed test specimen.

3. Numerical Simulations

To complement the experimental findings and attain deeper insights into the material's response under uniaxial and biaxial loading, finite element simulations were conducted. By combining the standardized testing procedures with advanced measurement techniques like DIC, this project aims to provide a comprehensive characterization of 7075-T6 aluminium's mechanical behaviour under uniaxial and biaxial loading conditions .

This section outlines the numerical methodology employed to simulate the tensile behaviour of a 7075-T6 Al alloy specimen using SolidWorks Simulation. The process follows a standard finite element (FE) framework, encompassing pre-processing, processing, and post-processing stages as illustrated in Fig. 6.

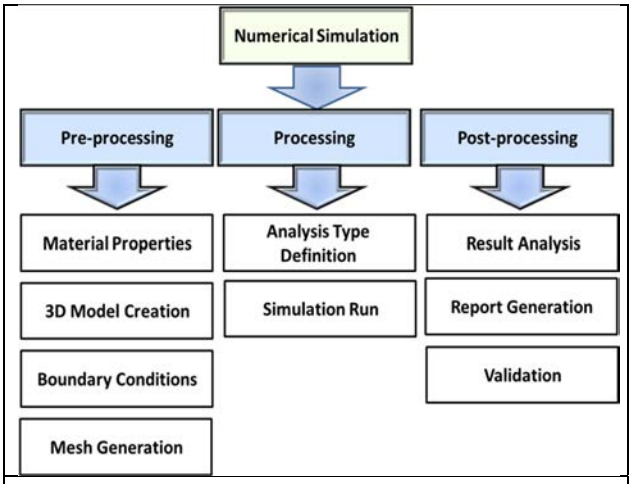

Fig 6. The process follows a standard finite element (FE) framework.

3.1. Pre-processing

This step comprises four key components including:

1. Material Properties: Essential material properties for the simulation, including density, Young's modulus, Poisson's ratio, yield strength, and ultimate tensile strength, are established from material testing data or relevant reliable literature.
2. 3D Model Creation: A precise 3D model of the tensile specimen, incorporating its exact geometry, dimensions, and any fillets, radii, or chamfers, is generated using SolidWorks software.
3. Boundary Conditions: Appropriate boundary conditions are applied, constraining one end of the specimen, and imposing a tensile load on the opposite end along the axial direction.
4. Mesh Generation: A refined mesh is created for the model to capture geometrical details and maintain numerical stability. The meshing strategy is chosen based on the complexity of the model and the desired level of accuracy.

3.2. Processing

This step is made up of following two key components :
1. Analysis Type Definition: The appropriate analysis type (e.g. linear static, nonlinear static, or dynamic) was selected based on the nature of the problem and the required accuracy.
2. Simulation Run: The simulation is run to determine the stress and strain distributions within the specimen under the applied load. This allows for the prediction of key mechanical properties such as ultimate tensile strength, and yield strength.

3.3. Post-processing

There are three key components to this step:
1. Result Analysis: The simulation outputs, including stress, strain, displacement, and other relevant parameters, were thoroughly analysed using SolidWorks simulation tools. This allows for a comprehensive understanding of the behaviour of 7075-T6 aluminium under the tensile load.
2. Report Generation: Detailed reports were generated, encompassing graphs, charts, and tables summarizing the simulation results .
3. Validation: The simulation results were validated by comparing them with experimental data or results obtained from alternative simulation tools. This step fosters confidence in the accuracy and reliability of the numerical predictions.

This structured approach ensures a robust FE framework for simulating the tensile behaviour of Al alloys within SolidWorks.

3.4. Numerical Analysis

This study investigates the failure behaviour of the 7075-T6 aluminium alloy using static finite element simulation in SolidWorks. The first step in building a numerical model was to create a 3D model of the specimen in the software, considering its exact geometry, dimensions and any fillets, radii or chamfers. Material properties, including density, Young's modulus, and Poisson's ratio were assigned and point loads of about 16100N and 20500N were applied. Fixed supports were defined as boundary conditions. The model was meshed with appropriate element size and type. The FE simulation was run using SolidWorks' FEM solver. Post-processing included analysing deformation and stress plots. Subsequently, mesh refinement was accomplished (according to Fig. 7 and Table 1). Mesh refinement refers to the process of gradually improving the resolution of a model by using increasingly finer meshes while comparing the results obtained from these different meshes. The simulation results provide insights into stress distribution and potential failure locations within the 7075-T6 model under the specified loads .
Enhancing mesh quality for accurate and efficient Al alloy simulations in SolidWorks offers numerous benefits. A finer mesh is used, leading to more accurate stress and displacement values, although a mesh convergence test and sensitivity analysis are performed to ensure that the mesh refinement is acceptable. Enhanced mesh accuracy in engineering simulations enables better design decisions, comprehensive analysis, early issue detection, and clearer visualization of results. This improved precision not only aids in identifying critical areas of stress and deformation but also facilitates effective communication among team members and stakeholders. Furthermore, a well-constructed mesh can reduce computation time, leading to faster simulations and more design iterations, ultimately resulting in a more efficient and optimized product development process. Details of the finite element model, such as the type of element, the size of the element and the number of nodes and elements, are given in Fig. 7. This optimization can result in lighter, stronger, and more efficient designs, leading to reduced material and manufacturing costs while improving overall performance. Overall, by implementing these improvements in mesh quality, engineers can achieve more accurate, efficient, and reliable simulations of 7075-T6 aluminium alloy in SolidWorks, ultimately leading to better product designs.

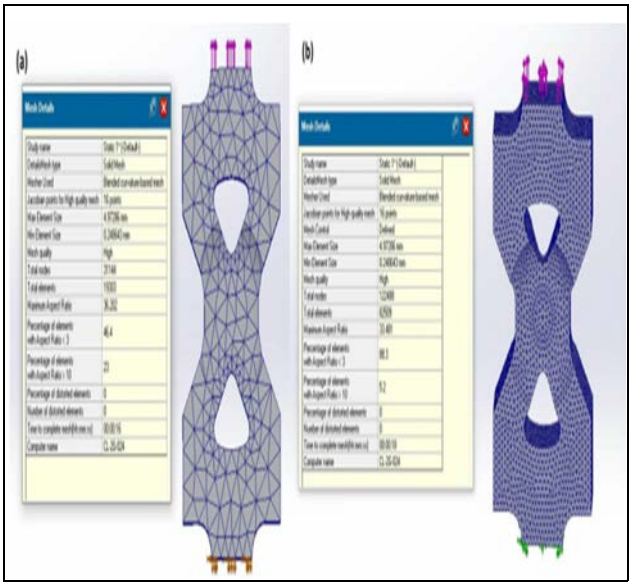

Fig 7. Test specimen model with (a) coarse mesh, (b) with refined mesh.

Table 1. Mesh comparison table

	Specimen model with coarse mesh	Specimen model with refined mesh
No of nodes	31144	122488
No of elements	19303	82508

4. Results and Discussion

4.1. Uniaxial/Biaxial Tensile Behaviour

Mechanical behaviour of metallic materials is a key factor in its durability during its performance cycle. It is worth indicating that there is a relation between various mechanical behaviour of the materials [25-26]. For example, the results of literatures have demonstrated that higher tensile strength generally exhibit improved fatigue resistance. Thus, the evaluation of mechanical behaviour of the 7075-T6 Al alloy such as tensile strength or the strain values under multidirectional loading can be beneficial to improve its performance. In this regard, analysis of the 3-point strain-time data for 7075-T6 aluminium alloy under a constant force of 16500 N with the given major and minor strains and time values are demonstrated in Table 2, Fig. 8, and Fig. 9. According to Table 2, the obtained results of major strains for 7075-T6 Al Alloy under 16500 (N) loading are 0.12, 0.02, and 0.05 which represent the primary deformation along the length of the material at three different points. The obtained values are positive, indicating elongation. In other words, 0.12 signifies a significant elongation of 12% at a specific point and 0.02 and 0.05 represent much smaller elongations of 2% and 5% respectively. The major strain values vary across the three points, signifying non-uniform elongation throughout the material due to the specimen's geometry. Furthermore, 7075-T6 has high yield strength, but the high major strain (0.12) at a relatively low force (16500 N) suggests possible plastic deformation at that specific point. This suggests that the material may exhibit some permanent elongation after the load is removed. It is worth mentioning that the magnitude of the major strain values can provide insights into the material's stiffness or elasticity at the applied force. Higher strain values indicate greater deformation under the same load.

On the other hand, the obtained minor strain of about 0.05, 0.001, and 0.001 represents the secondary deformation in directions perpendicular to the major strains. They are significantly smaller, indicating minimal deformation in the width direction.

The data indicates that the 7075-T6 aluminium alloy underwent significant elongation especially at one point (Point 1) of 0.12 or 12% under the constant load. The high strain and material properties suggest possible plastic deformation at that point.

Fig. 10 and Fig. 11 represent a set of 3 strain-time measurements taken on a 7075-T6 Al alloy specimen at a constant force of 20100 N as displayed in Table 2. The obtained data for major strains illustrates the larger principal strain experienced by the material at the time of measurement. The values are 0.011, 0.271, and 0.081, which indicate that the specimen experienced elongation (stretching) along the major strain axis. The result of minor strain represents the smaller principal strain experienced by the material at the time of measurement. The values are -0.081, 0.001, and 0.001, which indicates that the material is experiencing contraction (compressing) along the minor strain axis. It's worth noting that two of the minor strain values are very small, close to zero.

Given that all the measurements were taken at the same force and time, it suggests that multiple points on the same specimen were strained under the same conditions. The variation in the major strain values (0.011, 0.271, and 0.081) indicates that the material was not entirely uniform due to design geometry and/or the strain distribution was not perfectly even.

The minor strain values, especially the negative value, indicate that the material is compressing in a direction perpendicular to the major strain direction. It could be stated that both tests suggest the 7075-T6 aluminium alloy underwent significant elongation, particularly at some points. Moreover, Test 2 (20100 N) shows a much higher major strain value, indicating a stronger possibility of permanent deformation compared to Test 1 (16500 N).

Table 2. Tensile Test Results

3-Point Strain-Time Values under Force (16500N)			3-Point Strain-Time Values under Force (20100N)	
Selected point	**Major / Minor Strain**	**Time (s)**	**Major / Minor Strain**	**Time (s)**
Point 1	0.12 / 0.01	0-86	0.011 / -0.081	0-86
Point 2	0.02 / 0.001	0-86	0.271 / 0.001	0-86
Point 3	0.05 / 0.001	0-86	0.081 / 0.001	0-86

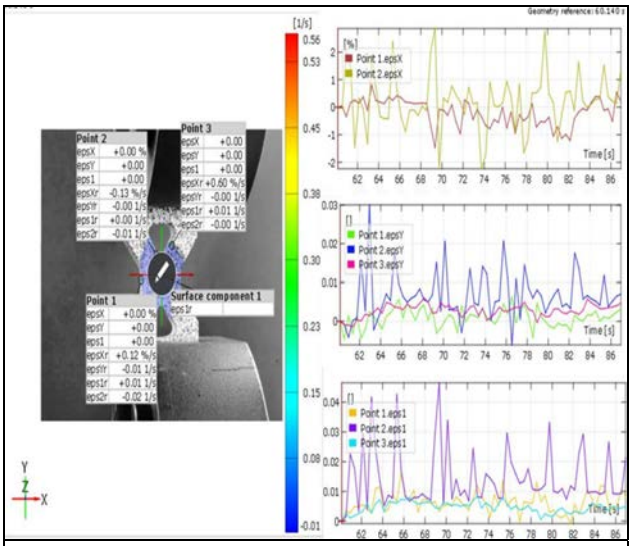

Fig 8. Major true strain of 3- point at force 16500N.

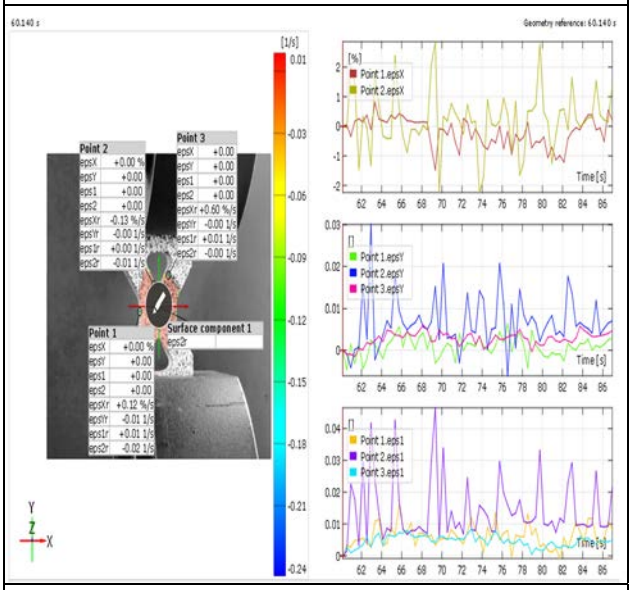

Fig 9. Minor true strain of 3-point at force 16500N.

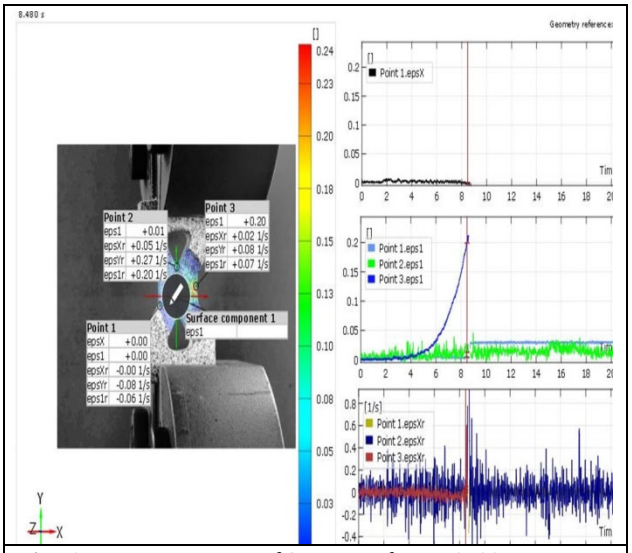

Fig 10. Major true strain of 3-point at force 20100N.

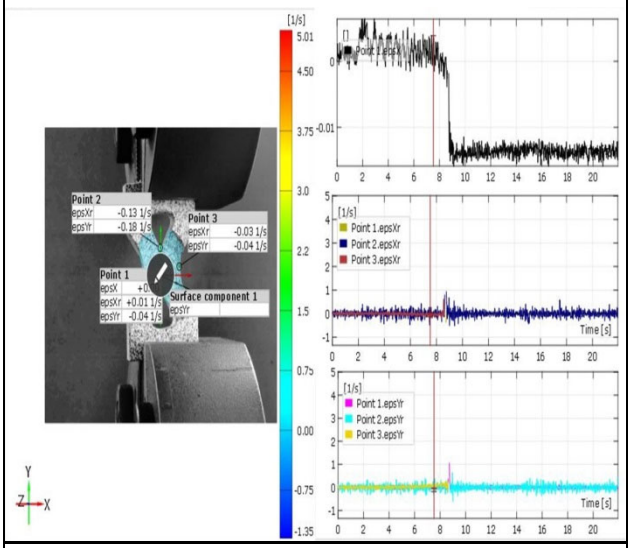

Fig 11. Minor true strain of 3-point at force 20100N.

4.1.1. Stress-Strain Behaviour Analysis of 7075-T6 Al

Fig. 12 (a) and (b) above are graphical representations of the DIC-derived stress-strain curves. The DIC analysis reveals linear elastic behaviour in 7075-T6 Al followed by plastic deformation beyond yield point. Increased applied force correlates with higher ultimate tensile strength (UTS) and yield strength (YS), suggesting strain hardening. Under uniaxial loading, significant necking indicates localized deformation, while a more gradual post-peak stress drop under biaxial loading suggests more uniform deformation.
This data informs advanced characterization of 7075-T6 for structural design applications.

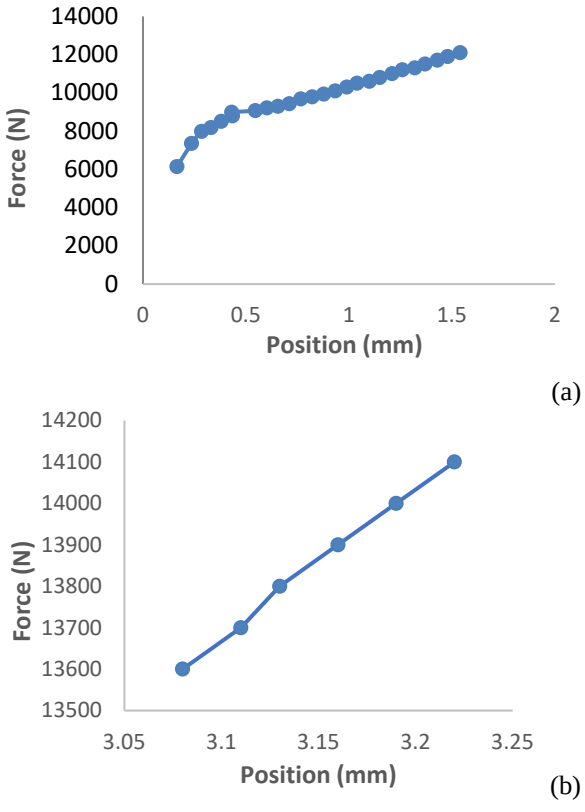

Fig 12. Stress-Strain curve under (a) force 16500N and (b) Stress-Strain curve at force 20100N**.**

5. CONCLUSION

Understanding the mechanical properties of 7075-T6 Al alloy such as obtained strains under uniaxial and biaxial loads is essential for optimization material design, failure analysis, and structural modelling. As the tensile strength is one of the key parameters affecting the fatigue strength, evaluation the behaviour of the material from this overview can be beneficial.

This investigation used DIC experiments together with numerical simulations to achieve these objectives, providing valuable insight into failure at applied forces of 16500N and 20100N.The combined experimental and computational approach revealed distinct failure modes in the material. Under uniaxial loading, localized necking and fracture were observed, while biaxial loading resulted in shear deformation and fracture. These findings highlight the importance of considering loading conditions in design of structures made from 7075-T6 Al. The study identified maximum principal stress and maximum shear stress as appropriate failure criteria for uniaxial and biaxial loading, respectively. These finding provide valuable information for the design and analysis of structures subjected to complex loading scenarios.

Confliction of Interest

The authors declare that they have no known competing financial interests or personal relationships that could have appeared to influence the work reported in this paper.

REFERENCES

[1] M.A. Alam, H.H. Ya, S.M. Sapuan, O. Mamat, B. Parveez, M. Yusuf, F. Masood, R.A. Ilyas, Recent advancements in advanced composites for aerospace applications: a review, Adv. Compos. Aerosp. Eng. Appl. (2022) 319–339. https://doi.org/10.1007/978-3-030-88192-4_16.

[2] A.T. Kermanidis, Aircraft aluminum alloys: applications and future trends, Revolutionizing Aircr. Mater. Process. (2020) 21–55. https://doi.org/10.1007/978-3-030-35346-9_2.

[3] M.T. Ali, Z. Jebri, J. Jumel, An enhanced surface treatment for effective bonding of 7075-T6 aluminium alloys, J. Adhes. (2024) 1–17. https://doi.org/10.1080/00218464.2024.2321263.

[4] A.V. Rex, S.K. Paul, A. Singh, Influence of uniaxial and equi-biaxial tensile pre-straining on the high cycle and notch fatigue behaviour of AA2024-T4 aluminium alloy, Theor. Appl. Fract. Mech. 128 (2023) 104176. https://doi.org/10.1016/j.tafmec.2023.104176.

[5] J.T. Burns, J.J. Jones, A.D. Thompson, J.S.W. Locke, Fatigue crack propagation of aerospace aluminum alloy 7075-T651 in high altitude environments, Int. J. Fatigue. 106 (2018) 196–207. https://doi.org/10.1016/j.ijfatigue.2017.09.017.

[6] M.M. Kadhim, S.K. Naif, D.F. Mohammed, A.W. Hussein, The concentration influence of multi-walled carbon nanotubes coating on fatigue edge crack growth and other mechanical properties of Al 7075-T6 thin plates, Results Eng. (2024) 102719. https://doi.org/10.1016/j.rineng.2024.102719 ·.

[7] M.Y. Khalid, R. Umer, K.A. Khan, Review of recent trends and developments in aluminium 7075 alloy and its metal matrix composites (MMCs) for aircraft applications, Results Eng 20 (2023), 101372, (n.d.). https://doi.org/10.1016/j.rineng.2023.101372.

[8] R.M. Nejad, F. Berto, M. Tohidi, Fatigue performance prediction of Al-alloy 2024 plates in riveted joint structure, Eng. Fail. Anal. 126 (2021) 105439. https://doi.org/10.1016/j.engfailanal.2021.105439.

[9] X. Zhang, Y. Chen, J. Hu, Recent advances in the development of aerospace materials, Prog. Aerosp. Sci. 97 (2018) 22–34. https://doi.org/10.1016/j.paerosci.2018.01.001.

[10] H. Zhu, J. Li, Advancements in corrosion protection for aerospace aluminum alloys through surface treatment, Int. J. Electrochem. Sci. (2024) 100487. https://doi.org/10.1016/j.ijoes.2024.100487.

[11] M.G.G. Camarinha, L.C. Campanelli, M.J.R. Barboza, L. Reis, A.A. Couto, D.A.P. Reis, Fatigue behavior of notched and unnotched 7075-T6 aluminum alloy subjected to retrogression and re-

aging (RRA) heat treatment and plasma nitriding, Theor. Appl. Fract. Mech. 127 (2023) 104051. https://doi.org/10.1016/j.tafmec.2023.104051.

[12] B.N. Sharath, D.G. Pradeep, K.S. Madhu, A Review on the Potential Impact of Age Hardening on Aluminium Alloys and Hybrid Composites for Engineering Applications, Prog. Eng. Sci. (2024) 100013. https://doi.org/10.1016/j.pes.2024.100013.

[13] A. Moradi, S. Ghorbani, M. Chizari, Experimental research on mechanical, material, and metallurgical properties of Inconel 600: Application in elevated temperature environment, J. Des. Against Fatigue. 2 (2024). https://doi.org/10.62676/jdaf.2024.2.1.30.

[14] J. Brnic, S. Krscanski, M. Brcic, L. Geng, J. Niu, B. Ding, Reliable experimental data as a key factor for design of mechanical structures, Struct. Eng. Mech. An Int'l J. 72 (2019) 245–256. https://doi.org/10.12989/sem.2019.72.2.245.

[15] D. Skejić, T. Dokšanović, I. Čudina, F.M. Mazzolani, The basis for reliability-based mechanical properties of structural aluminium alloys, Appl. Sci. 11 (2021) 4485. https://doi.org/10.3390/app11104485.

[16] M. Benedetti, C. Menapace, V. Fontanari, C. Santus, On the variability in static and cyclic mechanical properties of extruded 7075-T6 aluminum alloy, Fatigue Fract. Eng. Mater. Struct. 44 (2021) 2975–2989. https://doi.org/DOI: 10.1111/ffe.13530.

[17] X. Zhang, M. Yang, C. Zhou, N. Fu, W. Huang, Z. Wang, A review of in-plane biaxial fatigue behavior of metallic materials, Theor. Appl. Fract. Mech. 123 (2023) 103726. https://doi.org/10.1016/j.tafmec.2022.103726.

[18] J.C. Pang, S.X. Li, Z.G. Wang, Z.F. Zhang, General relation between tensile strength and fatigue strength of metallic materials, Mater. Sci. Eng. A. 564 (2013) 331–341. https://doi.org/10.1016/j.msea.2012.11.103.

[19] C. Gao, M.Q. Yang, J.C. Pang, S.X. Li, M.D. Zou, X.W. Li, Z.F. Zhang, Abnormal relation between tensile and fatigue strengths for a high-strength low-alloy steel, Mater. Sci. Eng. A. 832 (2022) 142418. https://doi.org/10.1016/j.msea.2021.142418.

[20] H. Mughrabi, Cyclic slip irreversibilities and the evolution of fatigue damage, Metall. Mater. Trans. B. 40 (2009) 431–453. https://doi.org/10.1007/s11663-009-9240-4.

[21] R. Liu, Y. Tian, Z. Zhang, X. An, P. Zhang, Z. Zhang, Exceptional high fatigue strength in Cu-15at.% Al alloy with moderate grain size, Sci. Rep. 6 (2016) 27433. https://doi.org/10.1038/srep27433.

[22] A.H. Siddiqui, P. Tiwari, J.P. Patil, A. Tewari, S. Mishra, Yield Locus and Texture Evolution of AA7475-T761 Aluminum Alloy under Planar Biaxial Loading: An Experimental and Analytical Study, J. Alloys Compd. (2024) 175115. https://doi.org/10.1016/j.jallcom.2024.175115.

[23] S. Hashemian, P.M. Keshtiban, A.E. haghi Oskui, Fracture behavior of the forged aluminum 7075-T6 alloy under mixed-mode loading conditions, Eng. Fail. Anal. 140 (2022) 106610. https://doi.org/10.1016/j.engfailanal.2022.106610.

[24] V. Chaves, G. Beretta, J.A. Balbín, A. Navarro, Fatigue life and crack growth direction in 7075-T6 aluminium alloy specimens with a circular hole under biaxial loading, Int. J. Fatigue. 125 (2019) 222–236. https://doi.org/10.1016/j.ijfatigue.2019.03.031.

[25] R. Nwawe, M. Grasso, Y. Chen, J. Klusak, & V. Rosiello, Optimisation of a gigacycle biaxial fatigue specimen for ultrasonic testing. Proceedings of Abstracts Engineering and Computer Science Research Conference 2019 (pp. 8–10). Hatfield, UK: University of Hertfordshire, (2019), DOI: 10.18745/pb.21692.

[26] P. Costa, R. Nwawe, H. Soares, L. Reis, M. Freitas, Y. Chen, D. Montalvão, Review of Multiaxial Testing for Very High Cycle Fatigue: From 'Conventional' to Ultrasonic Machines. Machines 2020, 8, 25. (2020) https://doi.org/10.3390/machines8020025.